Dossier

This paper is a part of the hereunder thematic dossier published in OGST Journal, Vol. 67, No. 1, pp. 5-178 and available online here

Cet article fait partie du dossier thématique ci-dessous publié dans la revue OGST, Vol. 67, n°1, pp. 5-178 et téléchargeable ici

DOSSIER Edited by/Sous la direction de : **F.H. Nader**

Diagenesis — Fluid-Rocks Interactions

Diagenèse minérale — Équilibres fluides-roches

Oil & Gas Science and Technology – Rev. IFP Energies nouvelles, Vol. 67 (2012), No. 1, pp. 5-178

IFP Energies nouvelles

Oil & Gas Science and Technology – Rev. IFP Energies nouvelles, Vol. 67 (2012), No. 1, pp. 77-95

DOI: 10.2516/ogst/2011173

Dossier
Diagenesis - Fluid-Rocks Interactions
Diagenèse minérale - Équilibres fluides-roches

Empirical Calibration for Dolomite Stoichiometry Calculation: Application on Triassic Muschelkalk-Lettenkohle Carbonates (French Jura)

M. Turpin[1#*], F.H. Nader[1] and E. Kohler[2]

1 Sedimentology-Stratigraphy Department, IFP Energies nouvelles, 1-4 avenue de Bois-Préau, 92852 Rueil-Malmaison Cedex - France
2 Geochemistry Department, IFP Energies nouvelles, 1-4 avenue de Bois-Préau, 92852 Rueil-Malmaison Cedex - France
 # Present address: Ruhr-University Bochum, Institute for Geology, Mineralogy and Geophysics, Sedimentary and Isotope Geology, Universitätstrasse 150, 44780 Bochum - Germany
e-mail: melanie.turpin@rub.de - fadi-henri.nader@ifpen.fr - eric.kohler@ifpen.fr

* Corresponding author

Résumé — Calibration empirique pour le calcul de la stœchiométrie de la dolomite : application aux carbonates triassiques du Muschelkalk-Lettenkohle (Jura français) — Cette étude propose une approche pour la quantification de la dolomite et le calcul de sa stœchiométrie grâce à l'utilisation de la diffraction des rayons X couplée aux affinements de maille et de Rietveld et complétée par de nombreuses données issues de la littérature. Elle permet d'obtenir une meilleure justesse et précision pour la quantification de la dolomite (et des autres phases minérales) ainsi que pour le calcul de sa stœchiométrie par rapport à l'équation de Lumsden et de méthodes antérieures. L'approche proposée est vérifiée grâce à l'analyse d'un échantillon référence de dolomite (Eugui) et appliquée à des roches carbonatées du Trias (Muschelkalk supérieur-Lettenkohle) du Jura français. Elle est combinée à une étude pétrographique et isotopique et peut être appliquée tant aux roches qu'aux ciments dolomitiques.

Les dolomies du Muschelkalk supérieur se sont formées au cours d'une dolomitisation d'enfouissement associée à des fluides dont la température augmente et ayant une composition isotopique variable au cours de l'enfouissement. Outre la pétrographie, ceci est également mis en évidence par le pourcentage de Ca calculé dans les dolomites, qui atteint progressivement une stœchiométrie idéale (de 53,16 % à 51,19 %) parallèlement au développement de la dolomitisation. Les dolomites du Lettenkohle montrent une stœchiométrie proche d'une stœchiométrie idéale (51,06 % Ca), sont ordonnées et associées à de l'anhydrite. Leur formation est liée à deux étapes de dolomitisation : de type sabkha et d'enfouissement.

Cette étude permet ainsi une meilleure caractérisation des différents types de dolomites dans les roches sédimentaires et par conséquent une meilleure détermination de leur potentiel en tant que réservoir.

Abstract — Empirical Calibration for Dolomite Stoichiometry Calculation: Application on Triassic Muschelkalk-Lettenkohle Carbonates (French Jura) — *This study concerns an approach for dolomite quantification and stoichiometry calculation by using X-ray diffractometry coupled with cell and Rietveld refinements and equipped with a newly substantial database of dolomite composition. A greater accuracy and precision are obtained for quantifying dolomite as well as other mineral phases and calculating dolomite stoichiometry compared to the classical "Lumsden line" and previous methods. The applicability of this approach is verified on dolomite reference material (Eugui) and on Triassic (Upper Muschelkalk-Lettenkohle) carbonates from the French Jura. The approach shown here is applicable to bulk dolostones as well as to specific dolomite cements and was combined with petrographical and isotopic analyses.*

Upper Muschelkalk dolomites were formed during burial dolomitization under fluids characterized by increased temperature and variable isotopic composition through burial. This is clear from their Ca content in dolomites which gradually approaches an ideal stoichiometry (from 53.16% to 51.19%) through increasing dolomitization. Lettenkohle dolostones consist of near-ideal stoichiometric (51.06%Ca) and well-ordered dolomites associated with anhydrite relicts. They originated through both sabkha and burial dolomitization.

This contribution gives an improved method for the characterization of different dolomite types and their distinct traits in sedimentary rocks, which allows a better evaluation of their reservoir potential.

INTRODUCTION

Ideal dolomite has a crystal lattice consisting of alternating layers of Ca and Mg, separated by layers of CO_3, and is typically represented by a stoichiometric chemical composition of $CaMg(CO_3)_2$ where calcium and magnesium are present in equal proportions (Reeder, 1990). Most of the properties of carbonate rocks (limestone and dolostone) are primarily defined during their deposition and subsequent early diagenesis. With reference to dolostones, rock properties tend to change with time and particularly so during mesogenesis (shallow marine to deep burial; Land, 1980). Commonly, these diagenetic stages represent an overprint of the previous depositional or early diagenetic events. Cation substitutions in the crystal lattice, in particular Ca and Mg, through dissolution-precipitation reactions, change the stoichiometry of the dolomite. As a result, dolomite exhibits variation in chemical composition and in atomic arrangements (Reeder, 1981; Hardie, 1987).

Very few sedimentary dolomites are truly stoichiometric ($CaMg(CO_3)_2$). They are better represented as:

$$Ca_{(1+x)}Mg_{(1-x)}(CO_3)_2$$

typically with more Ca than Mg (Goldsmith and Graf, 1958; Lumsden, 1979; Searl, 1994; Budd, 1997). Therefore, the term "dolomite" describes a mineral series of carbonate that encompass a range of chemical variation and lattice structures. The stoichiometry, the texture and possible association with evaporates are generally used to identify different types of dolomite in sedimentary rocks (Morrow, 1978, 1982a; Lumsden and Chimahusky, 1980). This can also reveal diagenetic environmental settings that affected dolomite formation (Mattes and Mountjoy, 1980; Morrow, 1982; Machel and Mountjoy, 1986). Non-stoichiometric dolomite crystals are thermodynamically metastable under sedimentary conditions and therefore more reactive to diagenetic environments relative to "ideal" dolomites (Carpenter, 1980; Land, 1980; Lumsden and Chimahusky, 1980; Hardie, 1987; Vahrenkamp and Swart, 1994; Chai *et al*., 1995; Budd, 1997). For this reason, a burial trend towards stoichiometry exists (Sperber *et al*., 1984; Vahrenkamp and Swart, 1994) resulting in an overall reset of stable isotope ratios and trace elemental abundances through recrystallization (Land, 1980; Morse and Mackenzie, 1990). By knowing the "degree" of stability of dolomites (through stoichiometry) a more quantitative prediction whether the dolomite rock texture is prone for further changes – that may alter its reservoir properties such as porosity and permeability – is feasible.

X-Ray Diffractometry (XRD) is commonly used for measuring the crystallographic structure and the stoichiometry of dolomites. The Ca/Mg ratio of a dolomite is classically determined from the displacement of the d_{104} main dolomite reflection. Lumsden (1979) established an equation linking molar content of $CaCO_3$ in dolomite to the d_{104} spacing measured on XRD profiles. Several authors have shown that dolostones can diverge from the Lumsden line (Reeder and Sheppard, 1984; Kimbell, 1993; Jones *et al*., 2001).

This paper presents an empirical calibration for the assessment of stoichiometry and crystal lattice properties of dolomite based on XRD peaks. Dolomite crystals lattice parameters ($a = b$ and c in Å in a rhombohedral crystal system) are determined by unit cell refinement, and by using a newly compiled database of dolomite composition. From these the related %Ca of the analyzed dolomites could be estimated. This approach yielded a better accuracy and precision than the previous methods. In addition, it is a rapid and inexpensive technique which only requires a small amount of sample. Hence, it allows for quantifying dolomite stoichiometry of bulk sediments as well as cements. This workflow also results in a mineralogical quantification of the coexisting phases in the samples based on the Rietveld refinement.

1 STUDY LOCALITY AND MATERIAL

The direct applicability of the presented approach is demonstrated on Triassic carbonates (Upper Muschelkalk and Lettenkohle Formation) from the Chatelblanc 1 borehole located in the French Jura *(Fig. 1)*. The Triassic is a period of transition associated with the beginning of the break-up of the Pangean supercontinent and the development of the Mesozoic basins. The Germanic facies province is characterized by a tripartite subdivision of the Triassic series (Ziegler, 1982) into the Scythian, the Anisian and Ladinian (including Muschelkalk carbonates and evaporates), and the Carnian to Norian (including Lettenkohle Formation). At the onset of the Late Ladinian, open-marine, clear water conditions induced the development of extensive carbonate platforms,

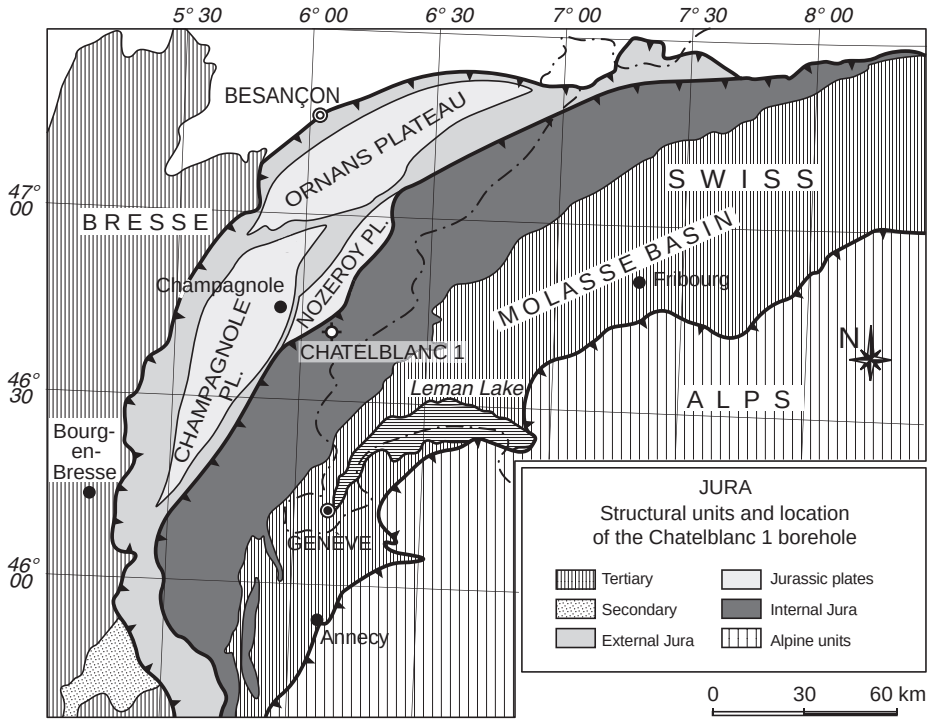

Figure 1

Simplified geological map of Jura structural units and location of the Chatelblanc 1 borehole.

these grade westwards and northwards into dolomitic and evaporitic clays (Wolburg, 1969; Senkowiczowa and Szyperko-Silwczynska, 1975; Alten *et al*., 1980). The Jura Mountain range is a small, arcuate fold belt forming the frontal portion and the youngest deformation zone (from Middle Miocene onward) of the northwestern Alpine arc surrounded by Tertiary basins *(Fig. 1)*. The Chatelblanc region is situated in the *Haute Chaîne Jura* of France *(Fig. 1)*. The landscape of this area consists of folded mounts with a general NE-SW direction. The Chatelblanc 1 borehole is located on an anticlinal axis NE-SW corresponding to the front of the *Haute Chaîne Jura* which overlaps the Nozeroy Plateau *(Fig. 1)*. The carbonate rock series of Upper Muschelkalk and Lettenkohle Formation are surrounded by two levels of decollement and are poorly or not affected by alpine compressive tectonic.

Forty carbonate samples from the Chatelblanc 1 borehole were collected from three core segments (No. 2, 3 and 4). Seventeen samples were taken from the Upper Muschelkalk (core segments 3 and 4 ranging from 2 289 m to 2 297 m depth), and twenty-three from the Lettenkohle Formation (core segment 2 ranging from 2 267 m to 2 277 m depth). The Upper Muschelkalk sedimentary rocks (limestones and dolostones) consist of mudstones, bioclastic wackestones and grainstones with rare evaporite nodules, while Lettenkohle sedimentary rocks are characterized by a succession of mudstones and evaporites (beds or displacive nodules of anhydrite) with some clay layers *(see Fig. 3 in Sect. 4.1.1)*. Their facies are characteristic of a shallow lagoon environment.

2 METHODS

2.1 X-Ray Diffractometry and Refinements

Each dry sample was uniformly ground in an agate mortar for XRD measurements. Alumina standard material (NIST) was added to each powder sample as an internal standard (50 wt%) and the mixture was again ground for few minutes until homogeneous. The Alumina cell parameters were taken from the NIST information file (SRM 676a). XRD patterns were collected using Cu radiation, from 0° to 80° 2θ with a 0.017° 2θ step size and 91 s. $2\theta^{-1}$ counting time with a position-sensitive detector on an X'pertPro Panalytical diffractometer. The identification of minerals was performed on the measured digitized diffractograms, using the ICDD database (PDF4+). XRD analyses in θ-2θ configuration were undertaken with a parallel beam focused by an elliptic W/Si crystal

mirror. The measurements were performed on the samples in holders (several g of powder) and also enclosed in a 1 mm glass capillary (0.1 g of powder).

Structure and cell refinements were performed on the resulting diagrams with HighScore Plus 2.2 software. The structure refinement method is based on a least-squares refinement procedure. This approach allows for a quantitative assessment of the agreement between observed and calculated integrated intensities by refining structural parameters (Rietveld, 1969). Based on all measured diffraction peaks, Rietveld refinement is used to quantify the relative proportions of coexisting phases in samples. Cell refinement was used to determine the unit cell parameters of the dolomite crystals. The peak positions of the NIST Alumina are used to correct the peak shift error (in two-theta) of the powder diagrams. The instrumental characteristics of the diffractometer, influencing peak shapes, have been taken into account for the refinement with Caglioti coefficients optimized ($U = 0.07509$, $V = -0.05312$ and $W = 0.03425$) on powder mineral standards (alumina, calcite, zinc oxide, quartz, molybdenite, muscovite). The relative error on quantification via Rietveld refinement was calculated for common minerals (Kohler *et al*., 2009). The uncertainty for non-clay phases is logically linked to the phase proportion in the sample. When the abundance is equal to 5%, the associated uncertainty is 60% while it decreases at 10% when the proportion is equal to 30%. Abundances higher than 40% are related to uncertainties less than 5%.

2.2 Petrography and Stable (C and O) Isotope Ratios

Samples were subjected to petrographic observations including conventional and cathodoluminescence (CL) microscopy (Cathodyne OPEA; operation conditions were 14 to 16 kV gun potential, 500 to 600 μA beam current, 0.05 torr vacuum).

The various carbonate (calcite and dolomite) phases (matrix and cements) were micro-sampled (using a dentist's micro-drill) for measuring their carbon and oxygen stable isotope composition. Analyses were carried out at the University of Erlangen, Germany. During this process, the carbonate powders were reacted with 100% phosphoric acid (density >1.9; Wachter and Hayes, 1985) at 75°C in an online carbonate preparation line (Carbo-Kiel – single sample acid bath) connected to a ThermoFinnigan 252 mass-spectrometer (Thermo Electron Corp., Waltham, MA, USA). All values are reported in per mill relative to Vienna Pee Dee Belemnite standard (V-PDB) by assigning a $\delta^{13}C$ value of +1.95‰ and a $\delta^{18}O$ value of −2.20‰ to National Bureau of Standards (NBS) 19. Oxygen isotopic compositions of dolomites were corrected using the fractionation factors given by Rosenbaum and Sheppard (1986). Reproducibility based on a replicate analysis of laboratory standards is better than ±0.02‰ for $\delta^{13}C$ and ±0.03‰ for $\delta^{18}O$.

3 EMPIRICAL APPROACH FOR STOICHIOMETRY ASSESSMENT OF DOLOMITES

3.1 Stoichiometry Calculation

A pioneering technique for the calculation of the dolomite crystal stoichiometry (%mol $CaCO_3$) was established by Lumsden (1979), who used the relationship between the calcium content and the measured d_{104} spacing on X-ray profiles. Calcium in excess of stoichiometry ($Ca_{50}Mg_{50}$) increases the d_{104} distance of dolomite as a linear function of the excess Ca amount (Goldsmith and Graf, 1958; Runnells, 1970; Lumsden, 1979). Lumsden (1979) used two d_{104} data points ($Ca_{50}Mg_{50}$ and $Ca_{55}Mg_{45}$) determined by Goldsmith and Graf (1958) to derive the linear relationship between d_{104} and composition: $N_{CaCO_3} = M \times d_{104} + B$ (with N_{CaCO_3}: $CaCO_3$ percent in dolomite, d: observed d_{104} value, $M = 333.33$ and $B = -911.99$). The standard error is ±0.15% on the mean composition with this procedure and the maximum difference for a given d_{104} value, based on the "Lumsden line", is about 1.45%Ca. Reeder and Sheppard (1984), Kimbell (1993) and Jones *et al*. (2001) reporting on the d_{104} value and the average %Ca (measured by electron microprobe) documented that Ca-rich dolostones differ significantly from the "Lumsden line" and could commonly deviate in the order of 4-5%Ca (Jones *et al*., 2001). These authors assign such discrepancies to a significant difference between the percentage of Ca atoms per formula unit determined by electron microprobe analysis and by XRD. Hence, Jones *et al*. (2001) have proposed a means of determining stoichiometries and abundances of dolomite phase based on a XRD peak fit method focusing on the d_{104} peak.

The study presented here develops an empirical calibration for calculating the dolostones stoichiometry based on the determination of the unit cell parameters of the dolomite crystals. It is based on the Rietveld technique, not solely on the dolomite main diffraction peak (d_{104}), as the classical Lumsden equation or as the peak fit method of Jones *et al*. (2001), but on several dolomite diffraction peaks. According to a unit cell refinement (crystal lattice deformation), this approach gives access to the lattice parameters of dolomite crystals ($a = b$ and c in Å). Using a new database of dolomite compositions as a function of lattice parameters allows calculating the %Ca in dolomites. This database is based on a comprehensive literature review. It is compiled from the crystallographic characteristics (cell parameters related to the lattice Ca percentage) of ninety-eight natural dolomites *(Tab. 1)*. Dolomites solely composed of Ca and Mg (no Fe and Mn, except for the well studied Eugui reference) have been considered in order to test the method in a simpler case study. Depending on the authors, stoichiometry of these natural dolomites has been determined by four distinct methods (X-ray refinement, electron microprobe analysis, X-ray fluorescence spectroscopy analysis, Lumsden equation; *Tab. 1*) associated with an own

TABLE 1 - PART 1

Crystallographic characteristics (cell parameters related to the lattice Ca and Mg percentages) of 98 natural dolomites. Dolomites only composed by Ca and Mg have been considered for this study (except the largely studied Eugui sample which contains also Fe and Mn). Stoichiometry of these dolomites has been determined by four distinct methods (X-ray fluorescence spectroscopy analysis, X-ray refinement, electron microprobe analysis, Lumsden equation). Authors, age and location of dolomite samples are also indicated

Dolomite studies	Age	Location sample	Method	$a = b$ (Å)	c (Å)	%mol Ca
Reeder and Wenk (1983)	Carboniferous	*Eugui, Spain*	XRF analysis	*4.8038*	*16.006*	*50.05*
Reeder and Sheppard (1984)	Carboniferous	*Eugui, Spain*	XRF analysis	*4.8078*	*16.002*	*50.06*
McCarty *et al*. (2006)	Carboniferous	*Eugui, Spain*	XRF analysis	*4.8086*	*16.0129*	*50.85*
McCarty *et al*. (2006)	Mississipian	Uinta County, USA	XRF analysis	4.8116	16.0251	51.35
McCarty *et al*. (2006)	Mississipian	Uinta County, USA	XRF analysis	4.8119	16.0278	51.35
McCarty *et al*. (2006)	Mississipian	Uinta County, USA	XRF analysis	4.8123	16.0238	52
McCarty *et al*. (2006)	Mississipian	Uinta County, USA	XRF analysis	4.8115	16.0311	52.05
McCarty *et al*. (2006)	Mississipian	Uinta County, USA	XRF analysis	4.8096	16.0213	51.65
McCarty *et al*. (2006)	Mississipian	Uinta County, USA	XRF analysis	4.809	16.0191	50.95
McCarty *et al*. (2006)	Mississipian	Uinta County, USA	XRF analysis	4.8104	16.0248	51.45
McCarty *et al*. (2006)	Mississipian	Uinta County, USA	XRF analysis	4.8095	16.0211	51.45
McCarty *et al*. (2006)	Mississipian	Uinta County, USA	XRF analysis	4.809	16.0139	50.7
McCarty *et al*. (2006)	Permian	Lea County, USA	XRF analysis	4.8127	16.0476	52.3
McCarty *et al*. (2006)	Permian	Lea County, USA	XRF analysis	4.8126	16.0455	52.4
McCarty *et al*. (2006)	Permian	Lea County, USA	XRF analysis	4.8137	16.0536	53.15
McCarty *et al*. (2006)	Permian	Lea County, USA	XRF analysis	4.813	16.0368	52.35
McCarty *et al*. (2006)	Permian	Lea County, USA	XRF analysis	4.8135	16.0517	52.5
McCarty *et al*. (2006)	Permian	Lea County, USA	XRF analysis	4.8129	16.0575	52.65
McCarty *et al*. (2006)	Permian	Lea County, USA	XRF analysis	4.8082	16.0101	50.3
McCarty *et al*. (2006)	Permian	Lea County, USA	XRF analysis	4.8083	16.0105	50.4
McCarty *et al*. (2006)	Permian	Lea County, USA	XRF analysis	4.8082	16.0077	50.1
McCarty *et al*. (2006)	Permian	Lea County, USA	XRF analysis	4.8089	16.015	50.6
McCarty *et al*. (2006)	Permian	Lea County, USA	XRF analysis	4.8123	16.0295	52.85
McCarty *et al*. (2006)	Permian	Lea County, USA	XRF analysis	4.8128	16.0364	52.85
McCarty *et al*. (2006)	Permian	Lea County, USA	XRF analysis	4.8144	16.0597	53.4
McCarty *et al*. (2006)	Permian	Lea County, USA	XRF analysis	4.8123	16.0391	52.4
McCarty *et al*. (2006)	Permian	Lea County, USA	XRF analysis	4.8126	16.0403	52.95
McCarty *et al*. (2006)	Permian	Lea County, USA	XRF analysis	4.8129	16.0459	52.85
McCarty *et al*. (2006)	Permian	Lea County, USA	XRF analysis	4.8122	16.0422	52.2
McCarty *et al*. (2006)	Permian	Lea County, USA	XRF analysis	4.813	16.0496	52.9
McCarty *et al*. (2006)	Permian	Lea County, USA	XRF analysis	4.814	16.0569	52.9
McCarty *et al*. (2006)	Permian	Lea County, USA	XRF analysis	4.8142	16.0595	53.4
McCarty *et al*. (2006)	Permian	Lea County, USA	XRF analysis	4.8138	16.0502	52.8
McCarty *et al*. (2006)	Permian	Lea County, USA	XRF analysis	4.8128	16.0458	52.9
McCarty *et al*. (2006)	Permian	Lea County, USA	XRF analysis	4.8157	16.0581	53.55
McCarty *et al*. (2006)	Permian	Lea County, USA	XRF analysis	4.8151	16.0506	53.15
McCarty *et al*. (2006)	Permian	Lea County, USA	XRF analysis	4.8136	16.0526	52.75
McCarty *et al*. (2006)	Permian	Lea County, USA	XRF analysis	4.8138	16.0498	53
McCarty *et al*. (2006)	Permian	Lea County, USA	XRF analysis	4.815	16.0586	53.4
McCarty *et al*. (2006)	Permian	Lea County, USA	XRF analysis	4.8122	16.06	52.5
McCarty *et al*. (2006)	Permian	Lea County, USA	XRF analysis	4.8134	16.0533	52.6
McCarty *et al*. (2006)	Permian	Lea County, USA	XRF analysis	4.8132	16.048	52.85
McCarty *et al*. (2006)	-	-	XRF analysis	4.8085	16.0113	50.8
McCarty *et al*. (2006)	-	-	XRF analysis	4.8111	16.0245	51.25
McCarty *et al*. (2006)	-	-	XRF analysis	4.8115	16.0266	51.55
McCarty *et al*. (2006)	-	-	XRF analysis	4.8119	16.0217	51.4
McCarty *et al*. (2006)	-	-	XRF analysis	4.8125	16.0312	52
McCarty *et al*. (2006)	-	-	XRF analysis	4.8122	16.0249	51.4

TABLE 1 - PART 2

Dolomite studies	Age	Location sample	Method	$a = b$ (Å)	c (Å)	%mol Ca
Reeder and Wenk (1983)	Carboniferous	*Eugui, Spain*	X-ray refinement	*4.8038*	*16.006*	*50.5*
Drits *et al*. (2005)	Permian	Lea County, USA	X-ray refinement	4.814	16.0411	54
Drits *et al*. (2005)	Permian	Lea County, USA	X-ray refinement	4.8274	16.1374	58.5
Drits *et al*. (2005)	Permian	Lea County, USA	X-ray refinement	4.8141	16.0392	53.5
Drits *et al*. (2005)	Permian	Lea County, USA	X-ray refinement	4.8247	16.1243	56.5
Drits *et al*. (2005)	Aptian	Coke County, USA	X-ray refinement	4.8114	16.025	53.5
Drits *et al*. (2005)	Aptian	Coke County, USA	X-ray refinement	4.8215	16.111	57
Althoff (1977)	-	Binnenthal, Switz.	X-ray refinement	4.8033	15.984	50.5
Navrotsky and Capobianco (1987)	Carboniferous	*Eugui, Spain*	EMP analysis	*4.8066*	*16.0016*	*50*
Goldsmith and Graf (1958)	-	*Lake Arthur, USA*	EMP analysis	*4.8069*	*16.0034*	*50.1*
Reeder (2000)	Eocene	Florida, USA	EMP analysis	4.8201	16.072	54.5
Reeder and Sheppard (1984)	Eocene	Florida, USA	EMP analysis	4.815	16.03	51.1
Reeder and Sheppard (1984)	Eocene	Florida, USA	EMP analysis	4.814	16.031	51.5
Reeder and Sheppard (1984)	Eocene	Florida, USA	EMP analysis	4.813	16.02	51.6
Reeder and Sheppard (1984)	Eocene	Florida, USA	EMP analysis	4.815	16.035	52.5
Reeder and Sheppard (1984)	Eocene	Florida, USA	EMP analysis	4.819	16.097	53.8
Reeder and Sheppard (1984)	Eocene	Florida, USA	EMP analysis	4.829	16.14	55.6
Reeder and Sheppard (1984)	Eocene	Florida, USA	EMP analysis	4.828	16.152	56
Reeder and Sheppard (1984)	Eocene	Florida, USA	EMP analysis	4.831	16.134	55.7
Reeder and Sheppard (1984)	Eocene	Florida, USA	EMP analysis	4.829	16.129	55.6
Reeder and Sheppard (1984)	Eocene	Florida, USA	EMP analysis	4.82	16.085	54.3
Reeder and Sheppard (1984)	Eocene	Florida, USA	EMP analysis	4.813	16.023	50.1
Reeder and Sheppard (1984)	Eocene	Florida, USA	EMP analysis	4.83	16.143	56.2
Reeder and Sheppard (1984)	Eocene	Florida, USA	EMP analysis	4.82	16.117	54.5
Reeder and Sheppard (1984)	Ordovician	Wisconsin, USA	EMP analysis	4.814	16.03	51.2
Reeder and Sheppard (1984)	Ordovician	Wisconsin, USA	EMP analysis	4.814	16.032	50.8
Reeder and Sheppard (1984)	Ordovician	Wisconsin, USA	EMP analysis	4.816	16.032	50.8
Reeder and Sheppard (1984)	Ordovician	Wisconsin, USA	EMP analysis	4.812	16.024	51.4
Spötl and Burns (1991)	Triassic	Austria	Lumsden equation	4.8032	16.0175	51
Spötl and Burns (1991)	Triassic	Austria	Lumsden equation	4.8076	15.9992	49
Spötl and Burns (1991)	Triassic	Austria	Lumsden equation	4.8056	16.0116	50.7
Spötl and Burns (1991)	Triassic	Austria	Lumsden equation	4.8035	16.0123	50
Spötl and Burns (1991)	Triassic	Austria	Lumsden equation	4.8048	16.0106	49
Spötl and Burns (1991)	Triassic	Austria	Lumsden equation	4.8066	16.0054	48.7
Spötl and Burns (1991)	Triassic	Austria	Lumsden equation	4.8047	16.0141	50
Spötl and Burns (1991)	Triassic	Austria	Lumsden equation	4.8077	16.0185	50
Spötl and Burns (1991)	Triassic	Austria	Lumsden equation	4.8038	16.0119	49
Spötl and Burns (1991)	Triassic	Austria	Lumsden equation	4.8062	16.0103	49.7
Spötl and Burns (1991)	Triassic	Austria	Lumsden equation	4.8053	16.0163	49.7
Spötl and Burns (1991)	Triassic	Austria	Lumsden equation	4.8033	16.0149	49.7
Spötl and Burns (1991)	Triassic	Austria	Lumsden equation	4.8047	16.0065	49.3
Spötl and Burns (1991)	Triassic	Austria	Lumsden equation	4.808	16.0205	50.3
Spötl and Burns (1991)	Triassic	Austria	Lumsden equation	4.8093	16.0226	51
Spötl and Burns (1991)	Triassic	Austria	Lumsden equation	4.8075	16.0302	51.7
Spötl and Burns (1991)	Triassic	Austria	Lumsden equation	4.806	16.0126	50.7
Spötl and Burns (1991)	Triassic	Austria	Lumsden equation	4.8091	16.0147	51.3
Spötl and Burns (1991)	Triassic	Austria	Lumsden equation	4.8057	16.0146	50.7
Spötl and Burns (1991)	Triassic	Austria	Lumsden equation	4.8053	16.0062	50
Spötl and Burns (1991)	Triassic	Austria	Lumsden equation	4.8051	16.0121	49.7

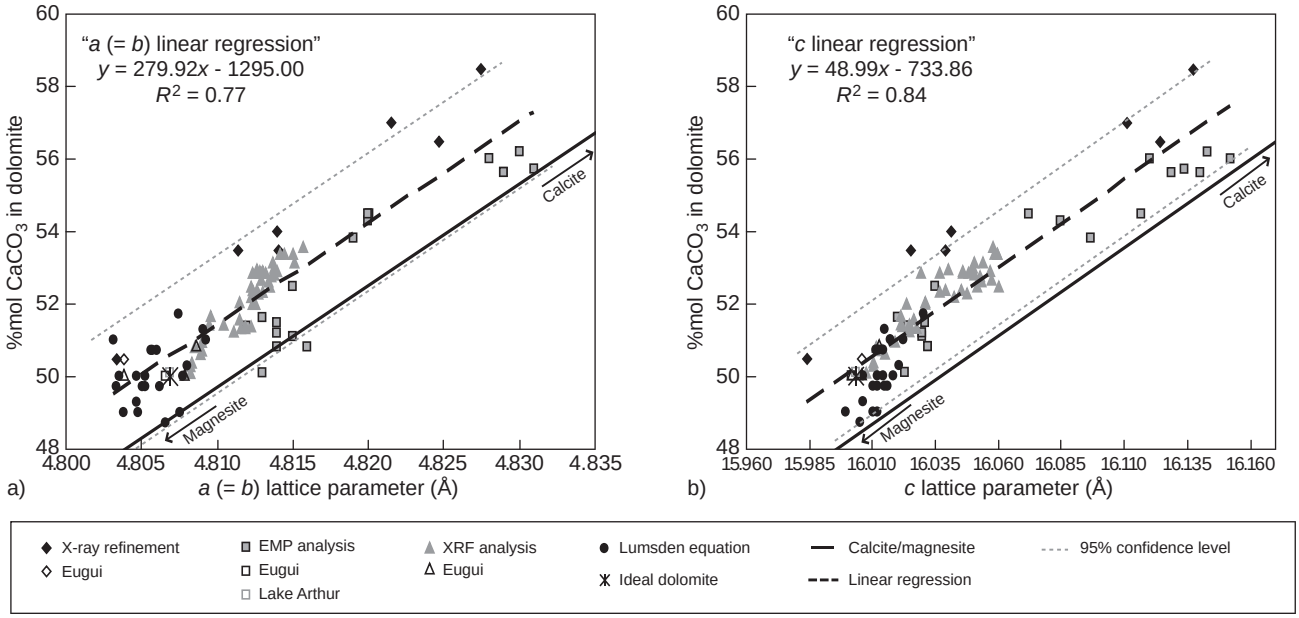

Figure 2

a (= *b*) lattice parameter value a) and *c* lattice parameter value b) linking the %mol $CaCO_3$ for 98 sedimentary dolomites *(see Tab. 1)*. Eugui and Lake Arthur dolomites represent ideally-ordered, single crystal specimens. Ideal dolomite characteristics are from Reeder (1990). The dark dashed line corresponds to calculated linear regression on dolomite samples selected in the literature. The dark solid line connects *a* (= *b*) or *c* lattice parameter values of magnesite and calcite. The grey dashed line symbolizes the uncertainty on the %$CaCO_3$ calculation using the linear regression at the 95% confidence level.

standard deviation on the %Ca calculation. Some of these studies include dolomites with a small %Ca range (Spötl and Burns; 1991; McCarty *et al*., 2006). However, they have been considered in order to propose an extensive database. From the collected data, two linear regressions can be calculated. A first one links the *a* (= *b*) crystallographic parameter to the %mol $CaCO_3$ in dolomite and a second one the *c* crystallographic parameter to the %mol $CaCO_3$ in dolomite *(Fig. 2)*.

A natural and nearly stoichiometric dolomite from the metamorphic carbonate complex of Eugui in Spain, extensively characterized (Barber *et al*., 1981; Reeder and Nakajima, 1982; Reeder and Wenk, 1983; Reeder and Markgraf, 1986; Navrotsky and Capobianco, 1987), was used as a comparative standard. This material is considered as ideally ordered with very few dislocations. The Eugui sample was used to test the reproducibility and the accuracy of the method proposed in this study for both lattice parameters refinement and stoichiometry calculation. The cell refinement analysis on the Eugui dolomite reference sample gives mean lattice parameters values of *a* (= *b*) = 4.8074(7) Å and *c* = 16.013(1) Å. The Eugui sample stoichiometry calculation based on the linear regressions from the database of dolomite compositions *(Fig. 2)* has a mean value of 50.69%Ca (50.70% on average based on the *a* (= *b*) equation and 50.69% on average based on the *c* equation). The electron microprobe analysis made on the Eugui sample provides a mean composition of 51.3%mol Ca, 47.3%mol Mg, 1.2%mol Fe and 0.2%mol Mn ($Ca_{1.03}Mg_{0.95}Fe_{0.02}Mn_{0.004}(CO_3)_2$). Analysis of the sample using the traditional Lumsden equation provides a mean value of 50.37%Ca. Barber *et al*. (1981), Reeder and Wenk (1983) and Jones *et al*. (2001) using other Eugui samples obtained a mean value of 50.4%Ca (Peakfit-XRD and EMP). Eugui sample analysis demonstrates that the uncertainty on the stoichiometry calculation using the approach presented in this study is related to the empirical calibration. The determination of lattice parameters values via the cell refinement is very accurate. It provides stoichiometry with a standard deviation estimated to be within ±0.05% and ±0.04% from *a* (= *b*) and *c* linear regressions respectively, and ±0.01% for the mean stoichiometry value from both linear regressions. The uncertainty related to the empirical calibration results in %Ca values deviating on average of ±1.90% and ±1.56% using *a* (= *b*) and *c* linear regressions respectively, at the 95% confidence level *(Fig. 2)*. Hence, the %Ca difference for Eugui sample between values determined by this procedure (50.70%) and by EMP (51.30%) in this study is thus within the uncertainty interval.

3.2 Comparison with Previous Studies

Jones *et al*. (2001) have developed a dolomite stoichiometry calculation based on a X-ray peak fit method on multi-phases dolomites. Lettenkohle and Upper Muschelkalk dolomites used here for application correspond to the matrix of dolostones. They are related to uniform and symmetrical diffraction peaks and do not show composite peak-forms (produced by the superposition of two peaks; see Jones *et al*., 2001 and Drits *et al*., 2005). If stoichiometric differences exist within samples (due to various populations of dolomite crystals), the difference is too small to be observed on the measured diffraction peaks of dolomite. Dolomites analyzed from Lettenkohle and Upper Muschelkalk are thus considered as mono-phase dolomites. It is feasible to determine the lattice parameters of multi-phases dolomites by cell refinement, however it couldn't be tested on the French Jura Triassic mono-phase dolomites. It is then difficult to compare accuracies on stoichiometry results from the Jones *et al*. (2001) method with the approach of the present study. However, Jones *et al*. (2001) looked only at the position and profile of d_{104} while the Rietveld and unit cell refinements used here are considering several dolomite diffraction peaks, providing a better accuracy and precision on results.

The study of McCarty *et al*. (2006) concerns dolomite stoichiometry and quantification of mono and two-phases samples using refinements on dolomite diffraction peaks. It also provides two linear equations relating *a* or *c* parameter to Ca content based on a combined X-ray, ICP-AES and XRF study. Based on the cell parameters values and the d_{104} peak position determined in the present study, stoichiometry of Eugui dolomite has been calculated with the Lumsden (1979) and the McCarthy *et al*. (2006) linear equations for comparison *(Tab. 2)*. As mentioned above, the stoichiometry of the Eugui sample of this study determined by microprobe is equal to 51.3%Ca. Stoichiometry calculated from the different linear equations show that the result from this study appears to be the closest value compared to the EMP value *(Tab. 2)*. It also emphasizes that stoichiometry is underestimated with the three different equations. Calculation of stoichiometry with the Lumsden equation exhibits the largest standard deviation (0.42%) while the lowest one is associated to the present study (0.1%). The stoichiometry value determined using either *a* (= *b*) or *c* equations is much more consistent in this study (absolute difference of 0.01% with a standard deviation of 0.02%) than using McCarthy *et al*. equations (absolute difference of 0.41% with a standard deviation of 0.18%). The calculations made in this study show that stoichiometry is always under-estimated based on the *a* (= *b*) equation compared to the *c* equation of McCarthy *et al*. (2006) while no rule is underlined using both equations from the present work. Uncertainty on stoichiometry calculation given in McCarthy *et al*. (2006) is lower than in the present study. However, calculation on Eugui shows that results from this work are more accurate and precise comparing to results based on McCarthy *et al*. (2006) equations *(Tab. 2)*.

The empirical calibration proposed in this study *(Fig. 2)* uses dolomites with negligible Fe and Mn while the Eugui dolomite reference sample and the Lettenkohle and Upper Muschelkalk dolomites do contain traces of Fe and Mn in their lattices. However, the %Ca calculated on Eugui dolomite by the approach presented here is consistent with the microprobe analysis and the previous studies (Barber *et al*., 1981; Reeder and Wenk, 1983; Jones *et al*., 2001). Therefore, this method can be equally applied to dolomites having few percent of Fe and Mn in their lattice. Care must be taken, however, when dolomites display higher Fe and Mn contents and tend toward the ankerite pole.

4 APPLICATION ON TRIASSIC CARBONATES OF THE FRENCH JURA

4.1 Characterization of Sediments

4.1.1 Mineral Quantification

The main components of Upper Muschelkalk sedimentary rocks are both dolomite and calcite *(Fig. 3)*. Quartz, feldspars, anhydrite, felsdpathoids and others minerals occur in minor or trace proportions. The main constituents of Lettenkohle sedimentary rocks are anhydrite and dolomite *(Fig. 3)*. These

TABLE 2

Mean stoichiometry value and Standard Deviation associated (SD) of Eugui sample calculated from different linear regression equations
The d_{104} position and the unit cell values are from this study

Eugui samples	d_{104} (Å)	$a = b$ (Å)	c (Å)	Ca (%mol) with a (= b)	Ca (%mol) with c	Mean %Ca	Linear regression equations from
Average SD	2.8871 0.0013	4.8074(7) 0.00025	16.013(1) 0.0013	50.70 0.07	50.69 0.06	50.69 0.01	This study
Average SD				50.16 0.11	50.57 0.08	50.37 0.02	McCarthy *et al*. (2006)
Average SD						50.37 0.42	Lumsden (1979)

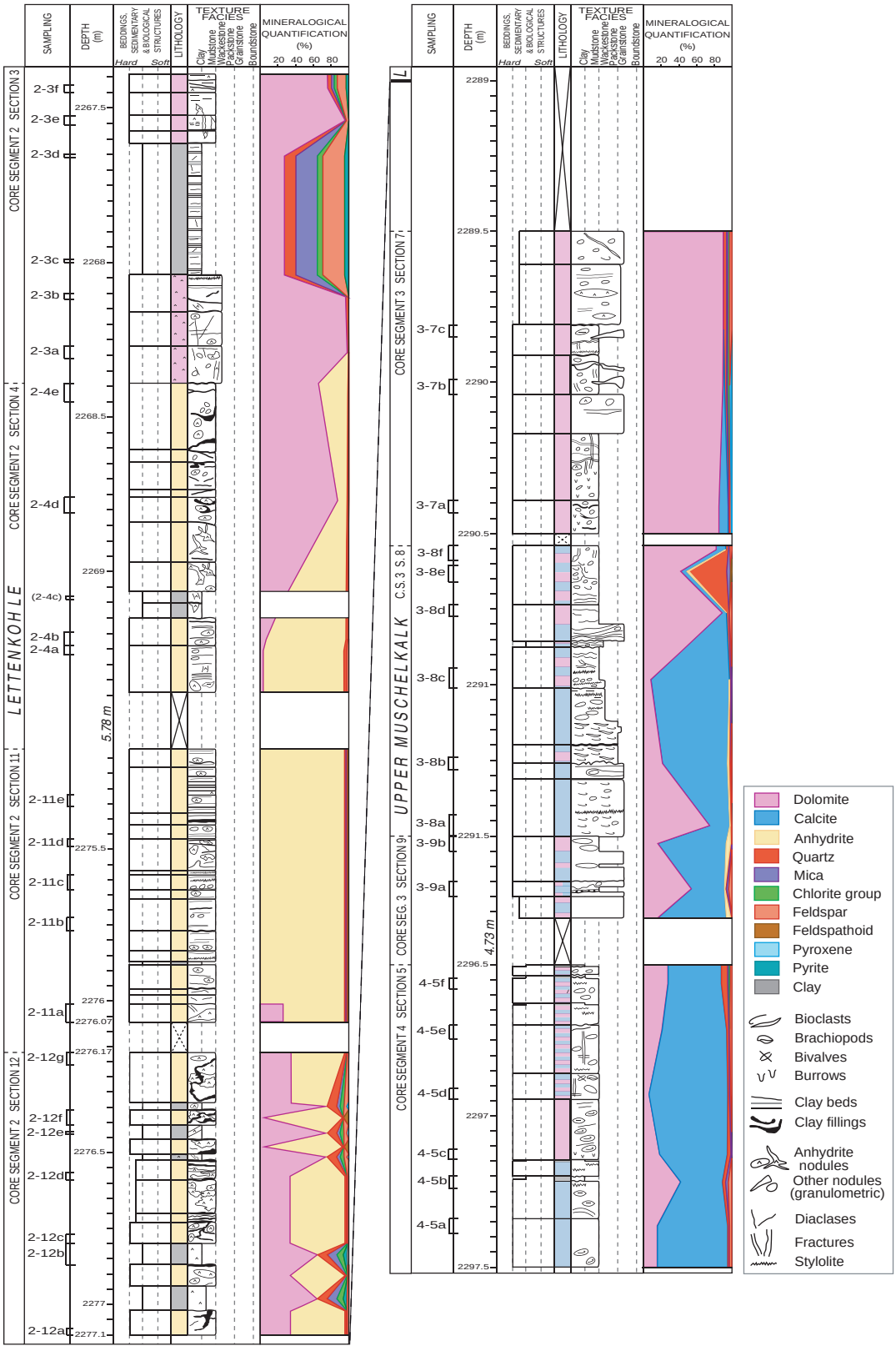

Figure 3

Detailed lithological log of the Upper Muschelkalk (core segments 3 and 4) and Lettenkohle Formation (core segment 2) of the Chatelblanc 1 borehole. Sampling, depth, structure and texture are indicated. Mineralogical quantification of limestones and dolostones is also given. Lithology is based on macroscopically observations while mineral quantification has been determined by X-ray diffractometry. The dashed line represents the log continuity with a gap in thickness indicated by depth values.

mineralogies alternate with intervals composed of quartz, feldspars, micas, chlorite group minerals and pyrite.

4.1.2 Petrographic Description and Paragenesis

The Upper Muschelkalk carbonate facies include two types of matrix (low-magnesium calcite and dolomite), three types of dolomite cements and three types of low-magnesium calcite cements *(Fig. 4, 5)*. The original lime-micritic matrix (CM) is completely or partially preserved in samples. Original calcite crystals form the foliated and prismatic structures of brachiopod shells whereas Calcite Cement 1 (CC1) is a mimetic replacement of precursor aragonite in bivalve shells *(Fig. 4b)*. Calcite Cement 2 (CC2) fills biomoldic pores *(Fig. 4e)* and also occurs in rare vugs. Calcite Cement 3 (CC3) fills fractures and occasionally veins *(Fig. 4d)*. The Dolomite Matrix (DM) is characterized by rhombs with an average size less than 20 μm, floating in the micritic limestone matrix *(Fig. 4)*. According to the classification proposed by Sibley and Gregg (1987), this dolomite is defined by a unimodal texture and euhedral (planar-e type) to subhedral (planar-s type) rhombs. Dolomite Cement 1 (DC1) consists of a unimodal planar-e texture with crystals size ranging from 15 to 75 μm *(Fig. 4c)*. Dolomite Cement 2 (DC2) occurs in biomolds and in rare vugs, is associated with CC2 *(Fig. 4e)* and defined by a polymodal texture and euhedral (planar-e type) crystals. Dolomite Cement 3 (DC3) is a blocky cement which fills fractures and rarely veins. It shows a polymodal planar-s texture composed by non-luminescent crystals with a size ranging from 50 to 1 500 μm. Fractures are filled either with CC3 or DC3 but never with both mineralogies. All dolomites have a mottled-red luminescence in CL except DC3. A relatively uniform Dolomite Matrix and two types of dolomite cements are distinguished in Lettenkohle sediments *(Fig. 5, 6)*. The Dolomite Matrix (DM) is defined by a unimodal texture and subhedral (planar-s type) rhombs, whose size is less than 20 μm. The matrix dolomite rhombs have a bright orange CL-pattern with a diffuse zonation (cloudy centres surrounded by clear rims; *Fig. 5a*). The Dolomite Cement 1 (DC1) occurs in rare vugs and has a polymodal planar-s texture composed by non-luminescent crystals with a size ranging from 15 to 150 μm *(Fig. 5b)*. The Dolomite Cement 2 (DC2) is characterized by a blocky cement type *(Fig. 5c, d)*. Dolomite crystals of this fracture-filling cement are defined by a polymodal planar-s texture, are non-luminescent under CL viewing and have sizes ranging from 50 to 1 500 μm.

The petrographic relationships between these various calcite and dolomite phases shed light on the relative timing of their formation *(Fig. 5)*. In the Upper Muschelkalk sedimentary rocks, the paragenesis proposed is based on the following arguments:

- the crosscutting of CC1 by DC1 suggests an early precipitation of CC1;
- the crosscutting of DC1 by CC2 indicates the previous occurrence of DC1;
- the corrosion of DC2 by CC2 favours an earlier precipitation of DC2;
- the crosscutting of all structures by fractures and veins, filled with CC3 or DC3, implies that they represent the latest carbonate precipitation.

Evidence for a chronology between CC3 and DC3 is lacking. In the Lettenkohle sedimentary rocks:

- the alternation of Dolomite Matrix (DM) and anhydrite (laminated macro- and microscopically) suggests their concomitant precipitation;
- the DM corrosion by anhydrite (irregular nodules macro- and microscopically) indicates a previous formation of the matrix;
- the crosscutting of all structures by the fractures and veins (except anhydrite with a regular nodule form macro- and microscopically), filled with DC2, suggests that DC2 represents the latest dolomite precipitation.

4.1.3 Description of Carbon and Oxygen Stable Isotopic Compositions

The isotopic ratios from well-preserved Middle Triassic brachiopods (low-magnesium calcite) represent the seawater composition (Korte *et al.*, 2005; *Fig. 7*). Marine dolomite $\delta^{18}O$ must not be directly compared with marine calcite $\delta^{18}O$ as the equilibrium fractionation between dolomite and water at low temperature is debatable (Land, 1980). A common method to avoid this problem is to calculate the equilibrium isotopic composition of calcite for a particular fluid and temperature, and then to assume a geologically reasonable value for $\Delta^{18}O_{dol\text{-}cal}$ (= $\delta^{18}O_{dolomite} - \delta^{18}O_{calcite}$ V-PDB), in order to derive an estimate of the equilibrium isotope composition of dolomite from that fluid at that temperature. A mean value of $\Delta^{18}O_{dol\text{-}cal}$ widely accepted to determine the marine dolomite signature, and applied here, is 3‰ (Budd, 1997; *Fig. 7*). Upper Muschelkalk isotope ratios show a fairly tight fit of both calcite and dolomite along a linear trend (correlation coefficient $R^2 = 0.66$) while Lettenkohle dolomite values are more variable. The $\delta^{18}O$ and $\delta^{13}C$ values of Calcite Matrix (CM) of the Upper Muschelkalk range from −6.2 to −2.2‰ and from 0 to +1.3‰ respectively, while calcite multi-phases samples (CM + CC1 + CC2) shows $\delta^{18}O$ values between −6.7 and −4‰ and $\delta^{13}C$ ratios from +0.2 to +1.1‰. Both matrix and multi-phase Upper Muschelkalk samples show the same covariance in $\delta^{18}O$ and $\delta^{13}C$. The Upper Muschelkalk calcite cement occurring as fracture infilling (CC3) lies off that covariant trend and shows lighter $\delta^{18}O$ (−8.0‰) and $\delta^{13}C$ (0‰) values. Muschelkak Dolomite Matrix (DM) displays $\delta^{18}O$ ratios from −7.8 to −3.8‰ and $\delta^{13}C$ between 0 and +1.3‰. The Upper Muschelkalk dolomite multi-phases samples (DM + DC1 + DC2) have $\delta^{18}O$ values ranging from −8.3 to −5.6‰ and $\delta^{13}C$ values between +0.2 and +1.1‰.

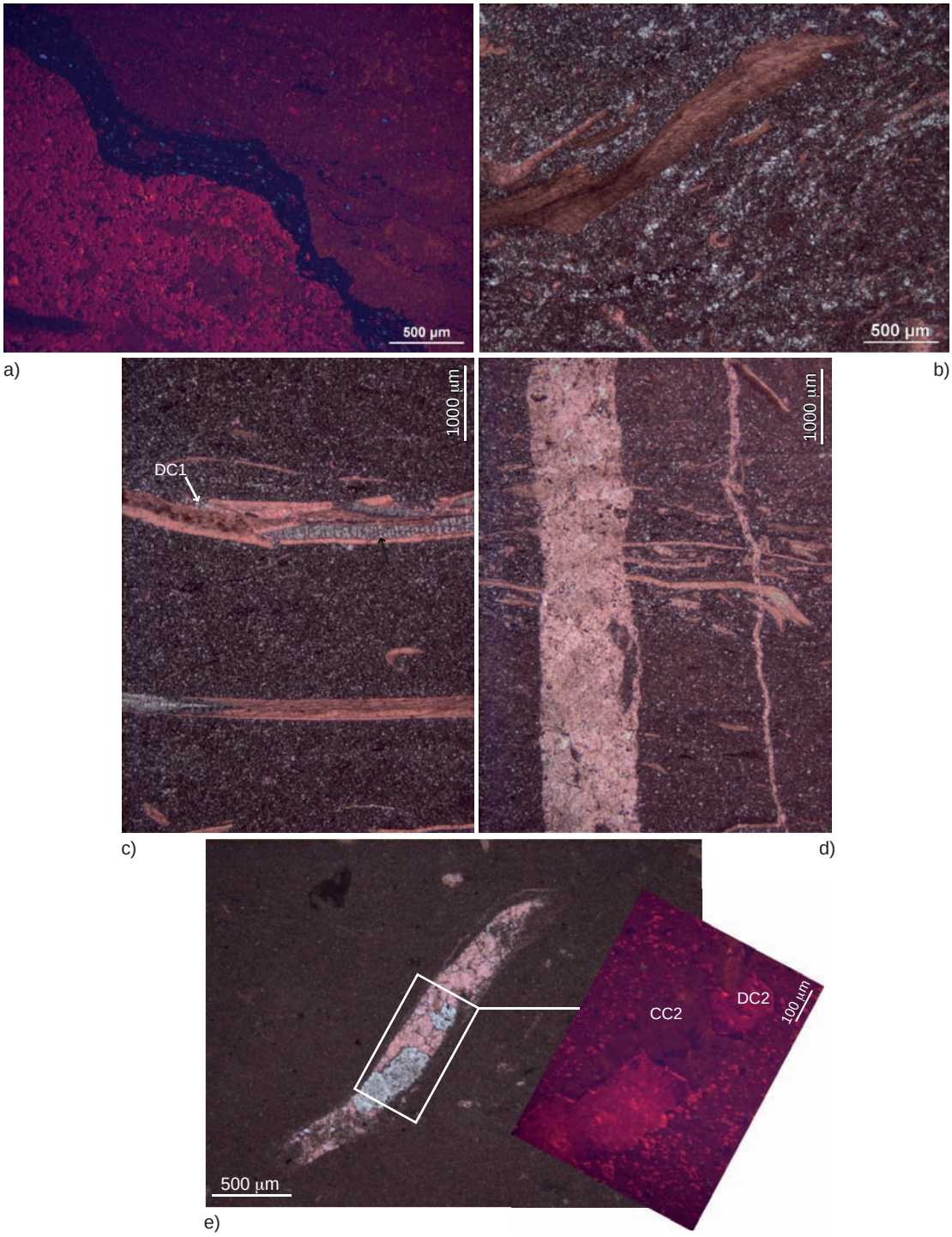

Figure 4

Transmitted light (coloured with alizarin red S and potassium ferricyanide) and CL photomicrographs of Upper Muschelkalk Chatelblanc 1 samples: a) CL photomicrograph of sample 3-8c showing the dull brown luminescent Calcite Matrix (CM) (top right), the Dolomite Matrix (DM) with a mottled red luminescence and bioclasts formed by the dull brown luminescent calcite (bottom left), separated by a stylolite filled by clays; b) plane-polarized photomicrograph of sample 3-8b showing the CM partially replaced by a DM and the Calcite Cement 1 (CC1) which mimics original bioclasts structure; c) plane-polarized photomicrograph of sample 4-5e showing the DM floating in the CM, the CC1, the Dolomite Cement 1 (DC1; white arrow) and biomold quartz filling (black arrow); d) plane-polarized photomicrograph of sample 4-5e showing CM, DM, CC1 and the blocky calcite cement (CC3) which fills fractures and veins; e) plane-polarized/CL photomicrograph-pair of sample 4-5a showing CM, the dull brown luminescent Calcite Cement (CC2) and the mottled red luminescent Dolomite Cement 2 (DC2) replacing the original bioclasts structure.

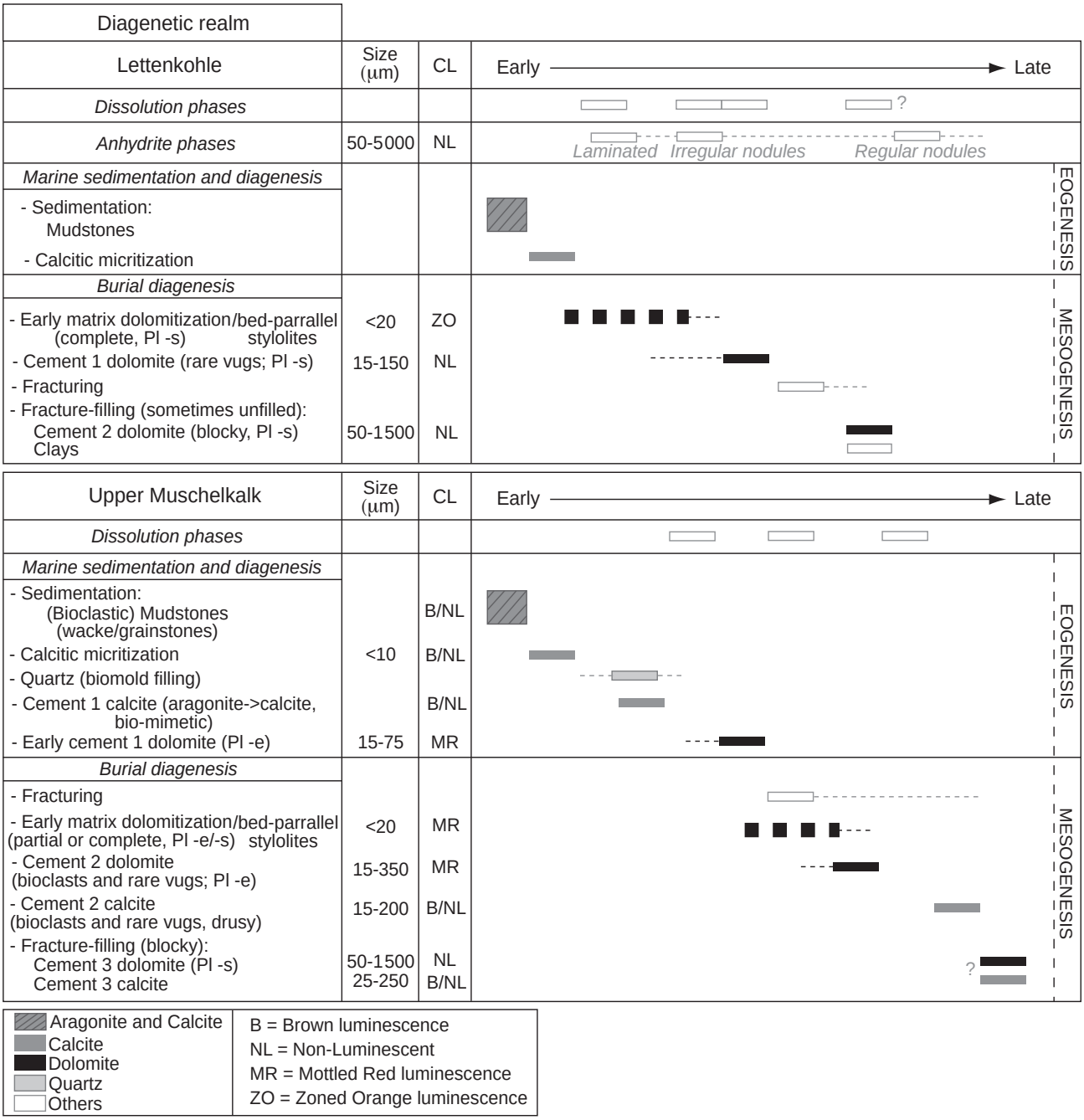

Figure 5

Paragenetic sequences of Upper Muschelkalk and Lettenkohle sediments. Grain size and CL pattern of matrix and cements are indicated.

Lettenkohle Dolomite Matrix (DM) shows $\delta^{18}O$ values ranging from –4.4 to –1.9‰ and $\delta^{13}C$ values between –2.6 and +0.1‰. A single fracture-filling Dolomite Cement 2 (DC2) displays more depleted $\delta^{18}O$ (–7.5‰) and $\delta^{13}C$ (–0.8‰) ratios.

4.2 Interpretation of Diagenetic Environments

The non-luminescent pattern of Upper Muschelkalk Calcite Matrix and Cements suggest that the fluids responsible of their precipitation were either oxidizing (hence no Mn^{2+} or Fe^{2+}

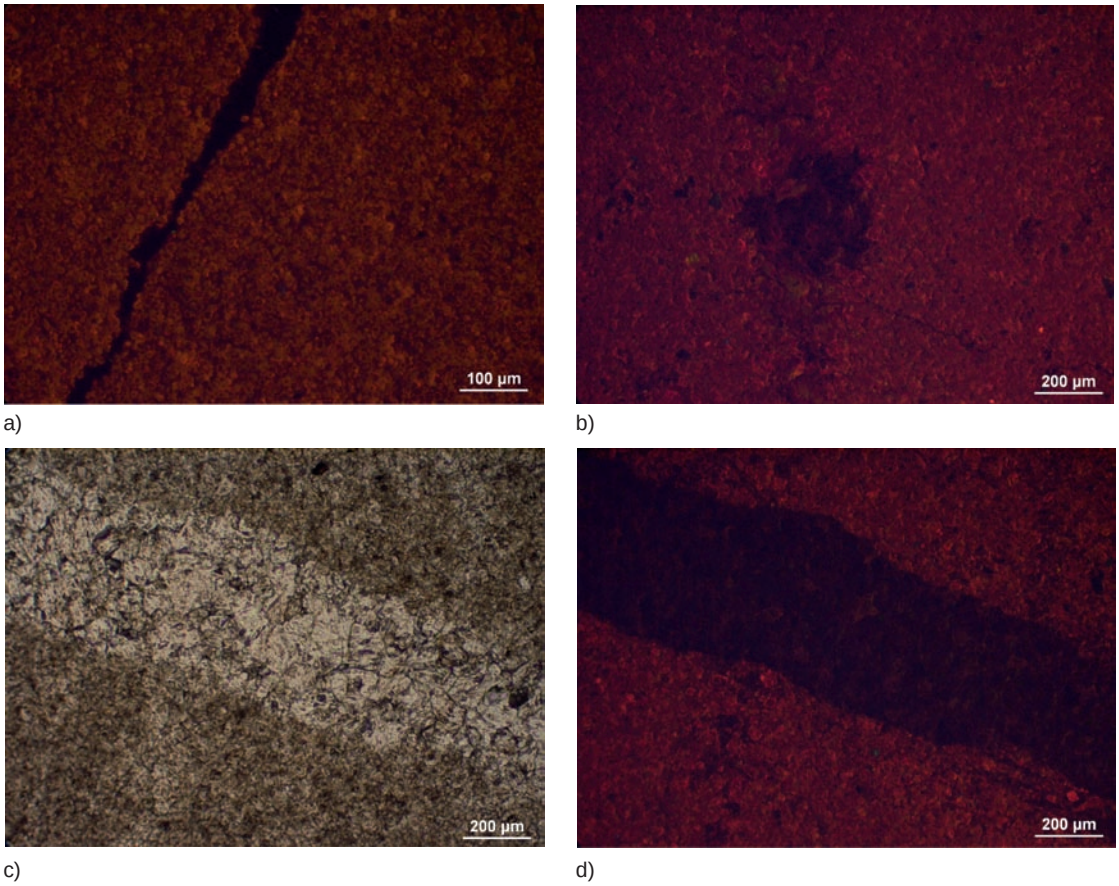

Figure 6

Transmitted light (coloured with alizarin red S and potassium ferricyanide) and CL photomicrographs of Lettenkohle Chatelblanc 1 samples: a) CL photomicrograph of sample 2-3b showing the Dolomite Matrix (DM) displaying a bright orange luminescence with cloudy centres surrounded by clear rims; b) CL photomicrograph of sample 2-3e showing the non-luminescent dolomite cement (DC1) in a vug; c, d) plane-polarized/CL photomicrograph-pair of sample 2-3e showing a non-luminescent blocky fracture-filling Dolomite Cement (DC2).

were available for incorporation into calcite), or were reducing but lacked a source of sufficient Mn^{2+} to generate a luminescent phase, and alternatively the fluids contained so much Fe^{2+} relative to Mn^{2+} that any luminescence generated is completely quenched. The $\delta^{18}O$ signature of some of these calcites (CM, CC1 and CC2) is close to reconstructed Triassic marine calcite compositions *(Fig. 7)*. This suggests that the fluid responsible for those precipitations most likely was seawater, at least for the calcite phases associated to the less depleted isotope values. Based on the paragenesis *(Fig. 5)*, the fracture fill cement (CC3) represents the latest precipitation in sediments. CC3 is associated to the lowest $\delta^{18}O$ value indicating formation from warm (hot?) waters during burial. The decrease in $\delta^{18}O$ *(Fig. 7)* could thus be associated to an increase of temperatures of precipitation during burial. The positive $\delta^{13}C$ values, close to the predicted paleo-seawater composition *(Fig. 7)*, suggest a local carbon source represented by the dissolution of marine carbonates. The decrease in $\delta^{13}C$ could be related to the increasing inputs of ^{12}C associated with organic matter alteration during burial. All of this results in a linear covariance in $\delta^{18}O$-$\delta^{13}C$ through burial. The mottled red luminescence of Upper Muschelkalk Dolomite Matrix and Cements (DC1 and DC2) indicates considerable amounts of Mn had to be present relative to Fe, pore waters had thus to be reducing. As dolomitization requires an ample Mg source, seawater could be the dolomitizing fluid. However, the dolomites are more depleted in $\delta^{18}O$ compared to the calcites and they differ substantially from the oxygen signature of predicted Triassic marine dolomites. If the dolomites are originated from seawater they should display a more enriched stable isotopic composition compared to the calcitic cements, which they do not *(Fig. 7)*. Consequently, the Upper Muschelkalk dolomites must be

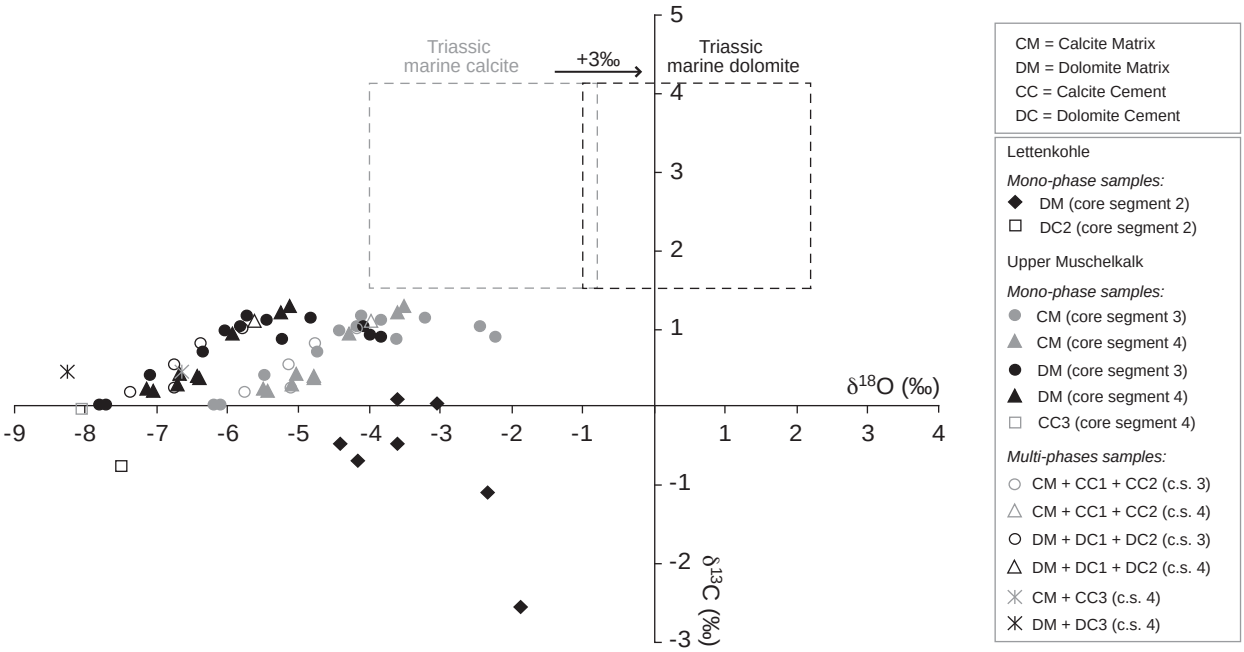

Figure 7

Carbon and oxygen isotope compositions of the various carbonate phases (dolomite/calcite, matrix/cement) of Upper Muschelkalk and Lettenkohle sedimentary rocks (present study). Grey dashed line square represents the isotopic values of well-preserved brachiopods (in low-magnesium calcite) precipitated from Middle Triassic seawater (Korte *et al*., 2005). Dark dashed line square symbolizes the predicted stable isotope record for dolomites precipitated with respect to the Triassic seawater ($\Delta^{18}O_{dol\text{-}cal}$ = +3‰; Budd, 1997).

the result of the circulation of burial fluids. As with the calcites, the linear trend in dolomite $\delta^{18}O$ values is interpreted to reflect increasing temperature with increasing burial as dolomitization proceeded.

In Lettenkohle rocks, the co-occurrence of dolomite and anhydrite suggests a dolomite formation in an evaporative environment. In such environments, ^{16}O is selectively removed by evaporation from the water body, so that the residual evaporated water is enriched in ^{18}O (Epstein and Mayeda, 1953; Lloyd, 1966). As a result, ^{18}O enriched values could indicate a dolomitization from higher salinity waters (Land, 1980). There is no simple relationship between isotopic composition and salinity, as interaction with the atmosphere and groundwater can decrease the degree of isotope enrichment (Major *et al*., 1992; Meyers *et al*., 1993) Fine-grained Lettenkohle dolomites (DM) do indeed have more positive $\delta^{18}O$ compositions and more variable $\delta^{13}C$ compositions compared to those of the Upper Muschelkalk matrix dolomites. Lettenkohle dolomite isotope values are more negative than what would even be expected for a dolomite from a Triassic seawater *(Fig. 7)*. This discrepancy can be explained by a diagenetic overprint. The Lettenkohle matrix dolomites exhibit a cloudy-centre-clear-rim texture. The cloudy centre often represents synsedimentary or early post-depositional dolomite precipitation, while the clear rims are the evidence of a continuing dolomite formation during burial (Machel, 2004; Choquette and Hiatt, 2008). Such overprinting during burial diagenesis would have also generated a decrease in the stable isotope signature of the Lettenkohle matrix dolomites relative to a purely evaporated seawater signal. In both Upper Muschelkalk and Lettenkohle sedimentary rocks, diagenetic conditions generate coarser dolomite crystals, as cements in fractures (DC3 in Upper Muschelkalk and DC2 in Lettenkohle) originated from a non original seawater fluid, characterized by an elevated temperature.

4.3 Dolomite Stoichiometry

Several types of Dolomite Matrix and Cements, associated to different crystal sizes, have been underlined by petrography *(Fig. 4-6)*. However, some carbonate phases couldn't be micro-sampled as a single phase explaining the distinction between mono- and multi-phase samples *(Fig. 7)*. For this reason, the stoichiometry calculated here is only associated to the Dolomite Matrix of samples. Only the DC2 in Lettenkohle have been micro-sampled as a single phase due to a sufficient amount of cement occurring in a large fracture (sample 2-3e).

The resulting stoichiometric calculations from empirical calibration *(Fig. 2)* show a distinction between dolomites of Upper Muschelkalk and Lettenkohle *(Tab. 3)*. Although

TABLE 3

Stoichiometry calculated on Upper Muschelkalk and Lettenkohle dolomites based on *a* (= *b*) and c linear regressions from this study. Three samples from Lettenkohle displaying inaccurate stoichiometry values between a (= *b*) and *c* equations due to low dolomite contents and not well-individualised dolomite diffraction peaks on X-ray profiles have been excluded (in grey). Although two samples in Upper Muschelkalk also show a low dolomite content, they are characterized by a better quality dolomite X-ray profile allowing to calculate an accurate stoichiometry with both *a* (= *b*) and *c* equations

Sample name	Dolomite (%)	*a* = *b* (Å)	*c* (Å)	Ca (%mol) with *a* (= *b*)	Ca (%mol) with *c*	Mean %Ca *a* and *c*
LETTENKOHLE						
2-3 f	76	4.8087 (5)	16.029 (0)	51.04	51.47	51.26
2-3 e	96	4.8080(2)	16.028(0)	50.85	51.42	51.13
2-3e (fracture)	100	4.8089(2)	16.026(9)	51.10	51.37	51.24
2-3 d	27	4.8081(7)	16.024(2)	50.90	51.23	51.06
2-3 b	97	4.8077(7)	16.022(4)	50.79	51.13	50.96
2-3 a	99	4.8088(4)	16.025(6)	51.07	51.32	51.20
2-4 e	66	4.8077(8)	16.022(2)	50.79	51.13	50.96
2-4 d	88	4.8091(0)	16.029(0)	51.13	51.47	51.30
2-4 b	7	4.8145(9)	16.015(3)	52.69	50.78	51.74
2-4 a	3	4.8237(1)	15.986(8)	55.24	49.41	52.33
2-11 a	26	4.8096(4)	16.037(0)	51.29	51.86	51.58
2-12 f	4	4.8116(2)	16.006(6)	51.85	50.39	51.12
2-12 e	74	4.8057(4)	16.011(4)	50.20	50.59	50.40
2-12 d	35	4.8069(4)	16.015(3)	50.54	50.78	50.66
2.12 b	26	4.8077(6)	16.021(1)	50.79	51.08	50.93
Average (core 2)		4.8081(2)	16.024(3)	50.87	51.24	51.06
Up. MUSCHELKALK						
3-7 c	90	4.8083(7)	16.028(0)	50.96	51.42	51.19
3-7 b	90	4.8092(2)	16.030(3)	51.18	51.52	51.35
3-7 a	85	4.8125(2)	16.045(0)	52.11	52.25	52.18
3-8 f	82	4.8118(9)	16.037(4)	51.94	51.86	51.90
3-8 e	42	4.8105(6)	16.044(7)	51.57	52.25	51.91
3-8 d	88	4.8115(4)	16.041(8)	51.83	52.11	51.97
3-8 c	8	4.8142(1)	16.038(0)	52.58	51.91	52.25
3-8 b	21	4.8124(6)	16.043(3)	52.11	52.16	52.13
3-8 a	74	4.8123(9)	16.046(2)	52.08	52.30	52.19
3-9 b	16	4.8145(4)	16.080(0)	52.67	53.97	53.32
3-9 a	54	4.8129(5)	16.047(4)	52.25	52.35	52.30
Average (core 3)		4.8118(8)	16.043(8)	51.93	52.19	52.06
4-5 f	26	4.8124(5)	16.048(7)	52.11	52.45	52.28
4-5 e	21	4.8153(9)	16.066(4)	52.92	53.28	53.10
4-5 d	6	4.8154(8)	16.067(9)	52.95	53.38	53.16
4-5 c	18	4.8136(0)	16.050(3)	52.53	52.50	52.51
4-5 b	41	4.8132(3)	16.055(4)	52.30	52.74	52.52
4-5 a	15	4.8135(7)	16.051(4)	52.41	52.55	52.48
Average (core 4)		4.8139(5)	16.056(7)	52.54	52.82	52.68
AVERAGE (3 & 4)		4.8126(1)	16.048(4)	52.15	52.41	52.28

Lettenkohle and Upper Muschelkalk Dolomite Matrix exhibit similar crystal sizes, Lettenkohle dolomites exhibit cell parameters and %mol $CaCO_3$ values smaller than values obtained for the Upper Muschelkalk dolomites. Cell parameters of Upper Muschelkalk dolomites from core segment 3 yield a mean %Ca of 52.06%. Muschelkalk dolomites from core segment 4 have higher cell parameters and thus a mean %Ca of 52.68%. Lettenkohle dolomites are associated to a mean stoichiometry of 51.06%Ca. Three samples in core segment 2 with low dolomite abundances (<7%) and poorly resolved dolomite peaks in X-ray profiles were not taken into account in the mean values of %Ca *(Tab. 3)*. The Lettenkohle sample, where the single Dolomite Matrix phase can be directly compared to the single Dolomite Cement phase DC2, shows that although they are related to different crystal sizes, they display similar stoichiometry values *(Tab. 3)*. In Upper Muschelkalk

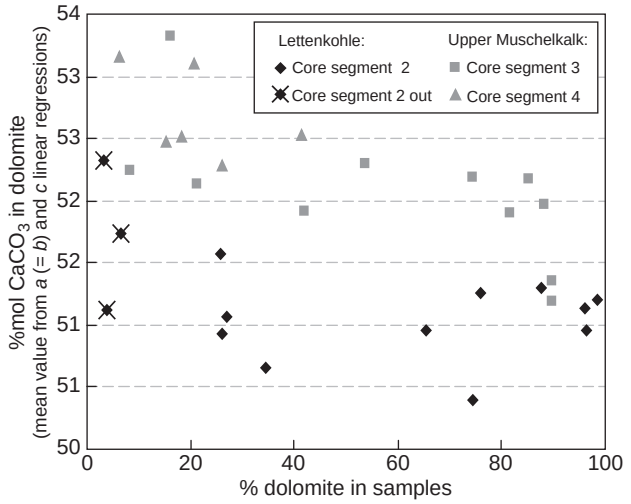

Figure 8

Dolomite stoichiometry (mean value based on *a* (= *b*) and *c* linear regressions) related to the dolomite content in Upper Muschelkalk and Lettenkohle sediments. The three Lettenkohle samples linked to inaccurate stoichiometry values are not considered *(see Tab. 2)*.

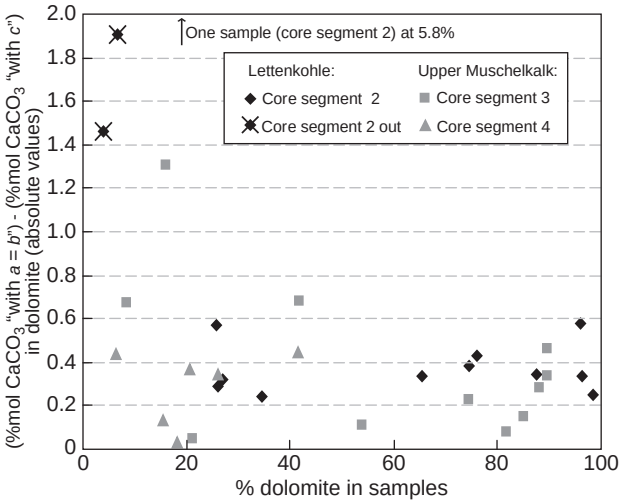

Figure 9

Calculated difference between the stoichiometries determined with *a* (= *b*) and *c* linear regressions depending on the dolomite content in Upper Muschelkalk and Lettenkohle sediments. The three Lettenkohle samples related to inaccurate stoichiometry values are not considered *(see Tab. 2)*.

sedimentary rocks, the abundance of dolomite in samples is correlated to the stoichiometry *(Fig. 8)*. When the dolomite amount increases in sediments dolomite is related to a lower %$CaCO_3$. However, such a trend is not as clear in the Lettenkohle samples *(Fig. 8)*. The stoichiometry calculation for Upper Muschelkalk and Lettenkohle dolostones is robust for a wide range of dolomite abundances *(Fig. 9)* as the difference between the stoichiometries calculated with the *a* (= *b*) and *c* linear regressions is in general smaller than 0.6%. This difference tends to get larger only when the dolomite abundance in sample is smaller than 6% *(Fig. 9)*. Upper Muschelkalk dolomites show higher and scattered lattice parameters (*a* = *b* and *c*) values than Lettenkohle dolomites, displaying lower and less variable lattice parameters *(Fig. 10)*. The deficiency of larger Ca ions in the unit cell of Lettenhkohle dolomites compared to Upper Muschelkalk dolomites is potentially a cause for the contraction in the a direction (see Rosen *et al.*, 1988). The expansion of the *c* parameter has been previously related to a cation disordering (Reeder and Wenk, 1983) or other lattice defects (Miser *et al.*, 1987). This is an explanation for the *c* variability of Upper Muschelkalk dolomites and could be caused by a faster crystallization (Rosen *et al.*, 1988) compared to Lettenkohle dolomites.

4.4 Dolomites and Reservoir Properties

The Upper Muschelkalk and Lettenkohle dolomites have their own properties *(Tab. 4)*. The near-ideal stoichiometry and the small variability of the *c* parameter in Lettenkohle dolomites

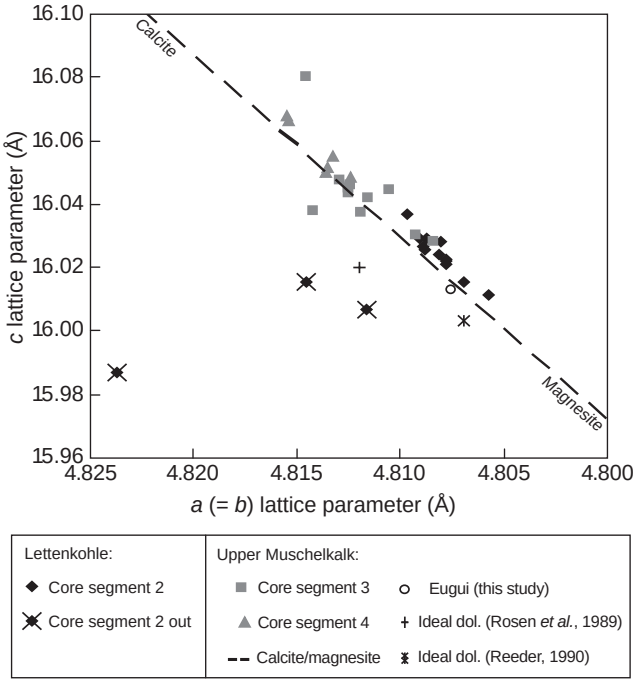

Figure 10

Unit cell dimensions of Upper Muschelkalk and Lettenkohle dolomites. The dark dashed line connects the unit cell values of calcite to magnesite. Ideal dolomites (from Rosen *et al.*, 1989; Reeder, 1990) are situated below this line due to the unit cell contraction when dolomite is well ordered. Eugui sample from this study is also indicated. The three Lettenkohle samples associated to inaccurate stoichiometry values are not considered *(see Tab. 2)*.

TABLE 4

Properties summary of Upper Muschelkalk and Lettenkohle dolomites of the Chatelblanc 1 borehole

Dolomites	Lettenkohle	Upper Muschelkalk
Unit cell parameters	a (= b) = 4.8081(2) Å c = 16.024(3) Å contracted in both a and c directions	a (= b) = 4.8126(1) Å c = 16.048(4) Å variable in both a and c directions
Stoichiometry	51.06 %mol $CaCO_3$	52.28 %mol $CaCO_3$
C and O stable isotopes	Matrix $\delta^{18}O = -3.30‰$ $\delta^{13}C = -0.75‰$ scattered values	Matrix $\delta^{18}O = -5.94‰$ $\delta^{13}O = 0.70‰$ linear trend (both matrix and cements)
CL pattern	Matrix bright zoned orange (NL for cements)	Matrix mottled red (mottled red + NL for cements)
Dolomitization	Sabkha type and burial	Burial
Diagenesis	Early burial	Early burial

(Fig. 10), associated with anhydrite, is in agreement with Warren (2000) proposing that dolomites formed in evaporite settings tends toward ideal stoichiometry and to a generally better ordered crystal lattice. Although Lettenkohle dolomites have undergone an early diagenetic overprint, they show a lower %$CaCO_3$ than Upper Muschelkalk dolomites probably due to their original evaporative environment of formation.

Upper Muschelkalk dolomites have been associated with a dolomitization during burial, marked by the %Ca of dolomites tending to ideal stoichiometry through dolomitization *(Fig. 8)*. In contrast, a sabkha model combined to a burial dolomitization are favoured for explaining Lettenkohle dolomite formation. Arguments that support the sabkha-related dolomitization are based on their near-perfect stoichiometry, their well-ordered lattice parameters and the occurrence of evaporite relicts, evidenced by nodular and displacive anhydrite *(Fig. 3, 10, Tab. 3)*. Shallow-water evaporative environments are associated with strong microbial activity, promoting dolomite precipitation and early dolomitization of other carbonates at low temperatures (Schreiber and El Tabakh, 2000). As a result of elevated salinity in these environments, calcite cementation of the associated deposits may not be prominent, as it is in normal marine settings and dolomite forms. This relation might explain the pervasive matrix dolomitization in Lettenkohle sediments which differs from Upper Muschelkalk sediments.

The dolomite recrystallization leads to the transformation of a non stoichiometric dolomite to a pure stoichiometric dolomite mineral in equilibrium with its pore fluids, including intermediate stages consisting of more disordered crystals (*i.e.* Ostwald ripening; Sibley *et al.*, 1994). This process commonly generates large crystals which grow at the expense of smaller ones (Morse and Casey, 1988; Nader *et al.*, 2004). Dolostone reservoir properties are related to their crystal size distributions, with more permeable dolostones being those consisting of overall larger crystals (Lucia, 1995). Therefore, in stable nearly stoichiometric sabkha-type dolomites, as Lettenkohle finely-crystalline dolostones, no further reservoir-enhancement is expected with burial and recrystallization. In contrast, reservoir properties of metastable poorly stoichiometric dolostones, originally composed of high Ca content dolomites, have the potential to improve with burial/recrystallization. However, on a larger scale, non stoichiometric dolomites could dissolve in one area and reprecipitate in another causing either porosity enhancement or porosity occlusion.

CONCLUSION

This paper documents an approach for the stoichiometry calculation of dolomites based on using linear regressions linking the %Ca and the unit cell parameters values ($a = b$ or c) obtained from a cell refinement on XRD profiles, also used for mineralogical quantification. Because mineral abundance and unit cell parameters determinations are not solely based on the d_{104} main dolomite diffraction peak, this approach allows quantification and stoichiometry calculation of dolomite with a better accuracy and precision relative to previous methods. The value and applicability of this method is directly demonstrated on Triassic reservoir rocks. The dolomite types from Upper Muschelkalk and Lettenkohle could be well distinguished by means of the stoichiometry calculation approach proposed in this contribution. Based on the stoichiometry level, the Upper Muschelkalk dolomites were prone to recrystallization during burial diagenesis, leading to increasing crystal sizes which potentially can enhance their reservoir quality. The originally near-stoichiometric, very finely crystalline, sabkha dolomites of Lettenkohle were less affected by recrystallization and remained with a lower reservoir quality, although they were

subjected to the burial diagenetic environment, as Upper Muschelkalk dolomites. Stoichiometry calculation can hence help in characterizing dolomites and draws ideas concerning their reservoir potentiality.

ACKNOWLEDGMENTS

M. Joachimski, Erlangen, Germany is acknowledged for stable isotopes analyses. A. Person and UPMC Mineralogy Collection are thanked for giving access to Eugui sample. We are grateful to A. Immenhauser for his helpful suggestions during the preparation of the manuscript. Comments on an earlier version of the manuscript by D.A. Budd and R.W. Luth are acknowledged. We are grateful to an anonymous reviewer for his constructive criticism of the manuscript. F. Ropital is thanked for the editorial handling of the manuscript.

REFERENCES

Barber D.J., Heard H.C., Wenk H.R. (1981) Deformation of Dolomite Single-Crystals from 20-800-Degrees-C, *Phys. Chem. Miner.* **7**, 6, 27-286.

Budd D.A. (1997) Cenozoic dolomites of carbonate islands: their attributes and origin, *Earth-Sci. Rev.* **42**, 1-47.

Carpenter A.B. (1980) The chemistry of dolomite formation I: the stability of dolomite, in *Concepts and Models of Dolomitization*, in: Zenger D.H., Dunham J.B., Ethington R.L. (eds), Special Publication Society of Economic Paleontologists and Mineralogists, pp. 111-121.

Chai L., Navrotsky A., Reeder R.J. (1995) Energetics of Calcium-Rich Dolomite, *Geochim. Cosmochim. Acta* **59**, 5, 939-944.

Choquette P.W., Hiatt E.E. (2008) Shallow-burial dolomite cement: a major component of many ancient sucrosic dolomites, *Sedimentology* **55**, 2, 423-460.

Dorobek S.L., Smith T.M., Whitsitt P.M. (1993) Microfabrics and geochemistry of meteorically altered dolomite in Devonian and Mississippian carbonates, Montana and Idaho, in *Carbonate Microfabrics*, Rezak R., Lavoie D.L. (eds), Springer-Verlag, New York, pp. 205-225.

Drits V.A., McCarty D.K., Sakharov B., Milliken K.L. (2005) New insight into structural and compositional variability in some ancient excess-Ca dolomite, *Can. Mineral.* **43**, 1255-1290.

Epstein S., Mayeda T. (1953) Variation of O-18 Content of Waters from Natural Sources, *Geochim. Cosmochim. Acta* **4**, 5, 213-224.

Goldsmith J.R., Graf D.L. (1958) Structural and compositional variations in some natural dolomites, *J. Geol.* **66**, 678-693.

Hardie L.A. (1987) Dolomitization: a critical view of some current views, *J. Sediment. Petrol.* **57**, 166-183.

Jones B., Luth R.W., MacNeil A.J. (2001) Powder X-ray diffraction analysis of homogeneous and heterogeneous sedimentary dolostones, *J. Sediment. Res.* **71**, 5, 790-799.

Kohler E., Parra T., Vidal O. (2009) Clayey cap-rock behavior in H_2O-CO_2 media at low pressure and temperature conditions: an experimental approach, *Clays Clay Minerals* **57**, 617-638.

Korte C., Kozur H.W., Veizer J. (2005) Delta C-13 and delta O-18 values of Triassic brachiopods and carbonate rocks as proxies for coeval seawater and palaeotemperature, *Palaeogeogr. Palaeoclimatol. Palaeoecol.* **226**, 3-4, 287-306.

Land L.S. (1980) The isotopic and trace element geochemistry of dolomite: the state of the art, in *Concepts and Models of Dolomitization*, Zenger D.H., Dunham J.B., Ethington R.L. (eds), Special Publication Society of Economic Paleontologists and Mineralogists, pp. 87-110.

Lloyd R.M. (1966) Oxygen Isotope Enrichment of Sea Water by Evaporation, *Geochim. Cosmochim. Acta* **30**, 8, 801-814.

Lumsden D.N. (1979) Discrepancy between Thin-Section and X-Ray Estimates of Dolomite in Limestone, *J. Sediment. Petrol.* **49**, 2, 429-436.

Lumsden D.N., Chimahusky J.S. (1980) Relationship between dolomite nonstoichiometry and carbonate facies parameters, in *Concepts and Models of Dolomitization*, Zenger D.H., Dunham J.B., Ethington R.L. (eds), Special Publication Society of Economic Paleontologists and Mineralogists, pp. 123-137.

Machel H.G. (2004) Concepts and models of dolomitization: a critical reappraisal, in *The geometry and petrogenesis of dolomite hydrocarbon reservoirs*, Rizzi C.J.R., Darke G. (eds), *Geol. Soc. London Spec. Publ.*, pp. 7-63.

Machel H.G., Mountjoy E.W. (1986) Chemistry and Environments of Dolomitization - A Reappraisal, *Earth-Sci. Rev.* **23**, 3, 175-222.

Major R.P., Lloyd R.M., Lucia F.J. (1992) Oxygen Isotope Composition of Holocene Dolomite Formed in a Humid Hypersaline Setting, *Geology* **20**, 7, 586-588.

Mattes D.H., Mountjoy E.W. (1980) Burial dolomitization of the Upper Devonian Miette buildup, Jasper National Park, Alberta, in *Concepts and Models of Dolomitization*, Zenger D.H., Dunham J.B., Ethington R.L. (eds), Special Publication Society of Economic Paleontologists and Mineralogists, pp. 259-297.

McCarty D.K., Drits V.A., Sakharov B. (2006) Relationship between composition and lattice parameters of some sedimentary dolomite varieties, *Eur. J. Miner.* **18**, 5, 611-627.

Meyers J.B., Swart P.K., Meyers J.L. (1993) Geochemical evidence for groundwater behavior in an unconfined aquifer, South Florida, *J. Hydrol.* **148**, 249-272.

Miser D.E., Swinnea J.S., Steinfink H. (1987) TEM Observations and X-Ray Crystal-Structure Refinement of a Twinned Dolomite with a Modulated Microstructure, *Am. Mineral.* **72**, 1-2, 188-193.

Morrow D.W. (1978) The influence of the Mg/Ca ratio and salinity on dolomitization in evaporite basins, *Bull. Can. Pet. Geol.* **26**, 389-392.

Morrow D.W. (1982) Diagenesis .1. Dolomite .1. the Chemistry of Dolomitization and Dolomite Precipitation, *Geosci. Can.* **9**, 1, 5-13.

Morse J.W., Casey W.H. (1988) Ostwald processes and mineral paragenesis in sediments, *Am. J. Sci.* **288**, 537-560.

Morse J.W., Mackenzie F.T. (1990) Geochemistry of Sedimentary Carbonates, *Developments in Sedimentology* **48**, 1-707, Elsevier, Amsterdam.

Nader F.H., Swennen R., Ellam R. (2004) Reflux stratabound dolostone and hydrothermal volcanism-associated dolostone: a two-stage dolomitization model (Jurassic, Lebanon), *Sedimentology* **51**, 339-360.

Navrotsky A., Capobianco C. (1987) Enthalpies of Formation of Dolomite and of Magnesian Calcites, *Am. Mineral.* **72**, 7-8, 782-787.

Reeder R.J. (1981) Electron optical investigation of sedimentary dolomites, *Contrib. Mineral. Petrol.* **76**, 148-157.

Reeder R.J. (ed.) (1990) *Carbonates: Mineralogy and Chemistry*, Mineralogical Society of America, *Rev. Mineral.* **11**, 399.

Reeder R.J., Markgraf S.A. (1986) High-Temperature Crystal-Chemistry of Dolomite, *Am. Mineral.* **71**, 5-6, 795-804.

Reeder R.J., Nakajima Y. (1982) The Nature of Ordering and Ordering Defects in Dolomite, *Phys. Chem. Miner.* **8**, 1, 29-35.

Reeder R.J., Sheppard C.E. (1984) Variation of Lattice-Parameters in Some Sedimentary Dolomites, *Am. Mineral.* **69**, 5-6, 520-527.

Reeder R.J., Wenk H.R. (1983) Structure Refinements of Some Thermally Disordered Dolomites, *Am. Mineral.* **68**, 7-8, 769-776.

Rietveld H.M. (1969) A Profile Refinement Method for Nuclear and Magnetic Structures, *J. Appl. Crystallogr.* **2**, 65-71.

Rosen M.R., Miser D.E., Starcher M.A., Warren J.K., (1989) Formation of Dolomite in the Coorong Region, South-Australia, *Geochim. Cosmochim. Acta* **53**, 3, 661-669.

Rosen M.R., Miser D.E., Warren J.K. (1988) Sedimentology, mineralogy and isotopic analysis of Pellet Lake, Coorong region, South Australia *Sedimentology* **35**, 1, 105-122.

Rosenbaum J., Sheppard S.M.F. (1986) An Isotopic Study of Siderites, Dolomites and Ankerites at High-Temperatures, *Geochim Cosmochim. Acta* **50**, 6, 1147-1150.

Runnells D.D. (1970) Errors in X-ray analysis of carbonates due to solid solution variation in the composition of component minerals, *J. Sediment. Petrol.* **40**, 1158-1166.

Schreiber B.C., El Tabakh M. (2000) Deposition and early alteration of evaporates, *Sedimentology* **47**, s1, 215-238.

Searl A. (1994) Discontinuous solid solution in Ca-rich dolomites: the evidence and implications for the interpretation of dolomitic petrographic and geochemical data, in *Dolomites: A volume in Honour of Dolomieu, International Association of Sedimentologists,* Special Publication, Purser B., Tucker M., Zenger D. (eds), pp. 361-376.

Senkowiczowa H., Szyperko-Sliwczynska A. (1975) Stratigraphy and palaeogeography of the Trias, *Geological Institute Bulletin Warsaw* **252**, 131-147.

Sibley D.F., Gregg J.M. (1987) Classification of dolomite rock texture, *J. Sediment. Petrol.* **57**, 967-975.

Sibley D.F., Nordeng S.H., Borkowski M.L. (1994) Dolomitization kinetics in hydrothermal bombs and natural settings, *J. Sediment. Res.* **64**, 3, 630-637.

Sperber C.M., Wilkinson B.H., Peacor D.R. (1984) Rock Composition, Dolomite Stoichiometry, and Rock Water Reactions in Dolomitic Carbonate Rocks, *J. Geol.* **92**, 6, 609-622.

Spötl C., Burns S.J. (1991) Formation of O-18-Depleted Dolomite within a Marine Evaporitic Sequence, Triassic Reichenhall Formation, Austria, *Sedimentology* **38**, 6, 1041-1057.

Vahrenkamp V.C., Swart P.K. (1994) Late Cenozoic dolomites of the Bahamas: metastable analogues for the genesis of ancient platform dolomites, *Dolomites: A volume in Honour of Dolomieu, in:* Purser B., Tucker M., Zenger D. (eds), International Association of Sedimentologists, Special Publication, pp. 133-153.

Warren J. (2000) Dolomite: occurrence, evolution and economically important associations, *Earth-Sci. Rev.* **52**, 1-3, 1-81.

Ziegler P.A. (1982) Triassic Rifts and Facies Patterns in Western and Central-Europe, *Geol. Rundschau* **71**, 3, 747-772.

Final manuscript received in October 2011
Published online in February 2012